# SUPPLEMENTARY INFORMATION

## Polar-Nonpolar Oxide Heterostructures for Photocatalysis

**I. The calculations of band edge alignment by GGA+U and HSE.**

The band edge alignment should be calculated correctly in order to compare the redox potentials of $H_2O$ with CBM and VBM of the designed oxide heterostructures. We first study STO(001) surface as a test. It is known that for STO surface, $V_{H^+/H_2}$ and $V_{O_2/H_2O}$ are located within the band gap.[1-2]A slab consisting of 4 layers SrO and 5 layers $TiO_2$ is used as shown in Fig. S1 (a). We found that although GGA+U calculation gives a reasonable band gap, it does not yield the correct band edge alignment. In comparison, HSE gives a reasonable results for both band gap and band edge alignment. Considering that HSE calculation is very time-consuming, we use HSE functional to calculate DOS shown in Fig.3, in order to make a correct comparison with $H_2O$ redox potentials. The other properties are calculated using GGA+U.

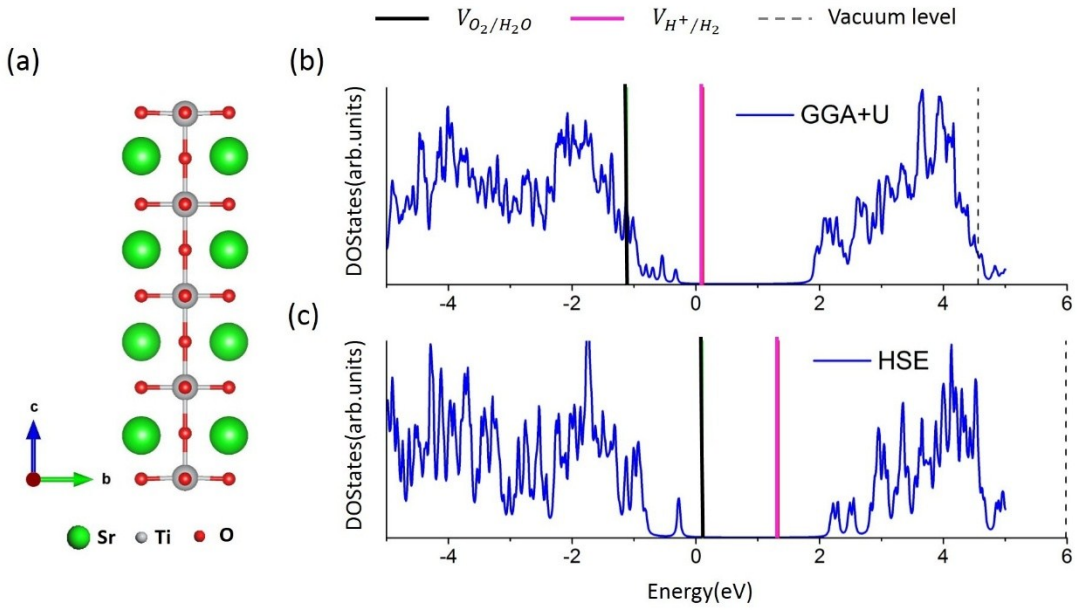


**Figure S1** Atomic structure (a) and DOS of STO slab calculated by GGA+U (b) and HSE functional (c). The redox potentials of $H_2O$ is marked by the black and pink lines. The vacuum level is marked by the dashed line.

**II. The band structure of n-p-type STO/LAO/STO heterostructures with different terminations.**

n-p-type STO/LAO/STO (001) heterostructures has an indirect band gap. Fig. S2 presents the band structures of SrO-SrO, SrO-$TiO_2$, $TiO_2$-SrO and $TiO_2$-$TiO_2$ heterostructures with 5 uc LAO. One can see that SrO-SrO has the largest indirect band gap and is insulating

with 5 uc LAO. However, if we compare the band structures with the absorption intensity (Fig.3 (a)), we found that the low energy absorption peaks are associated with the direct band gap. $TiO_2$-SrO heterostructure has the largest band gap with very low absorption below 1eV. SrO-$TiO_2$ heterostructure has the strongest absorption, corresponding to its smallest direct band gap. (Table S2).

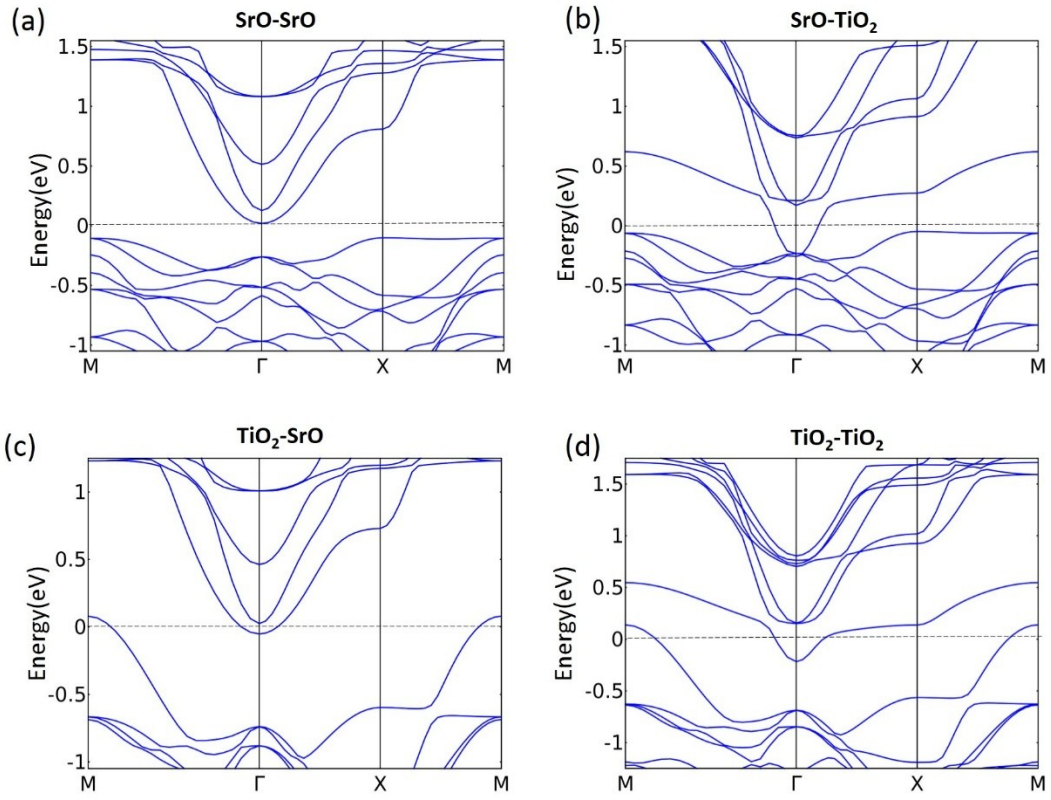


**Figure S2** Band structures of SrO-SrO, SrO-$TiO_2$, $TiO_2$-SrO and $TiO_2$-$TiO_2$ heterostructures with 5uc LAO.

| | SrO-SrO | SrO-$TiO_2$ | $TiO_2$-SrO | $TiO_2$-$TiO_2$ |
|---|---|---|---|---|
| Indirect band gap (eV) | 0.12 | -0.21 | -0.13 | -0.36 |
| Direct band gap at Γ point(eV) | 0.28 | -0.02 | 0.71 | 0.47 |

**Table.S1** Indirect and direct band gap at Γ point of SrO-SrO, SrO-$TiO_2$, $TiO_2$-SrO and $TiO_2$-$TiO_2$ heterostructures with 5uc LAO.

## III. The orbital distribution of CB and VB.

The VB is contributed by O-2p band and the nature of CB depends on the termination. As shown in Figure S3, For the SrO-SrO and $TiO_2$-SrO terminations, the CB is dominated by *dxy* orbital. For SrO-$TiO_2$ and $TiO_2$-$TiO_2$ terminations, CB is a mixture of all *t2g* orbitals.

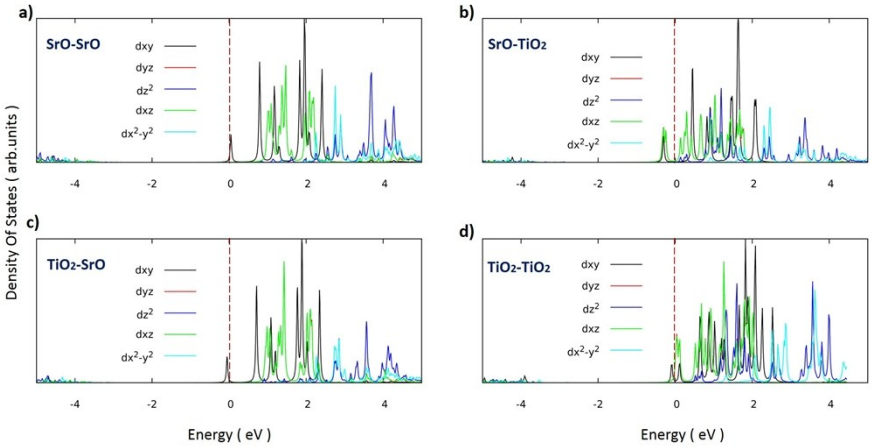


Figure S3. The partial DOS of CB for n-p type STO/LAO/STO with different terminations.

## IV. The light absorption coefficient of n-p STO/LAO/STO heterostructures in different directions and in comparison with bulk STO.

Compared to $SrTiO_3$ bulk, there would be an additional absorption peak appearing at 0.2-0.5 eV region when LAO thickness exceeds 4ucs for SrO-$TiO_2$ type (Fig. S4 (a)), this is associated with the decreasing band gap with the increasing LAO thickness. For other types, the behaviors are similar. Fig. S4 (b) compares the absorption coefficient between xy and z direction (taking 4-6uc LAOs into account), one can see that the peaks at the low energy region for xy direction (black, green, pink curves) are lower than those for z direction (red, dark blue, light blue curves) (about 0.4 eV lower), indicating that xy direction has a stronger absorption. So we show absorption coefficient of xy direction for all the cases in the main text.

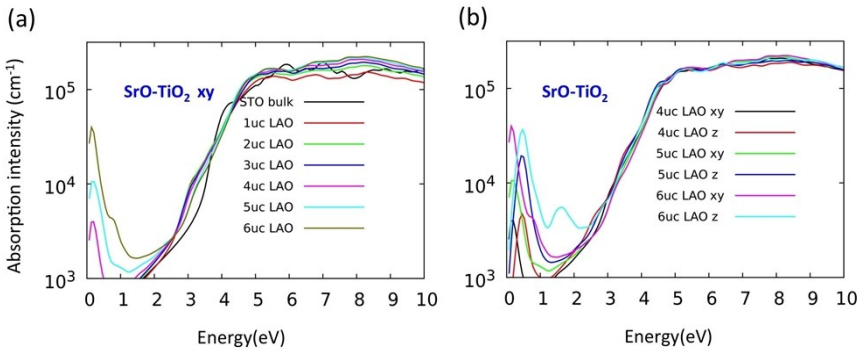


**Figure S4** light absorption of SrO-$TiO_2$ heterostructures with different unit cells LAO in different directions.

## V. The energy alignment with respect to $H_2O$ redox potentials of n-p STO/LAO/STO with 5 ucs LAO.

All the band alignments are very close to those with 3 ucs LAO, hence we can conclude that the applicability of the heterostructure is independent of LAO thickness.

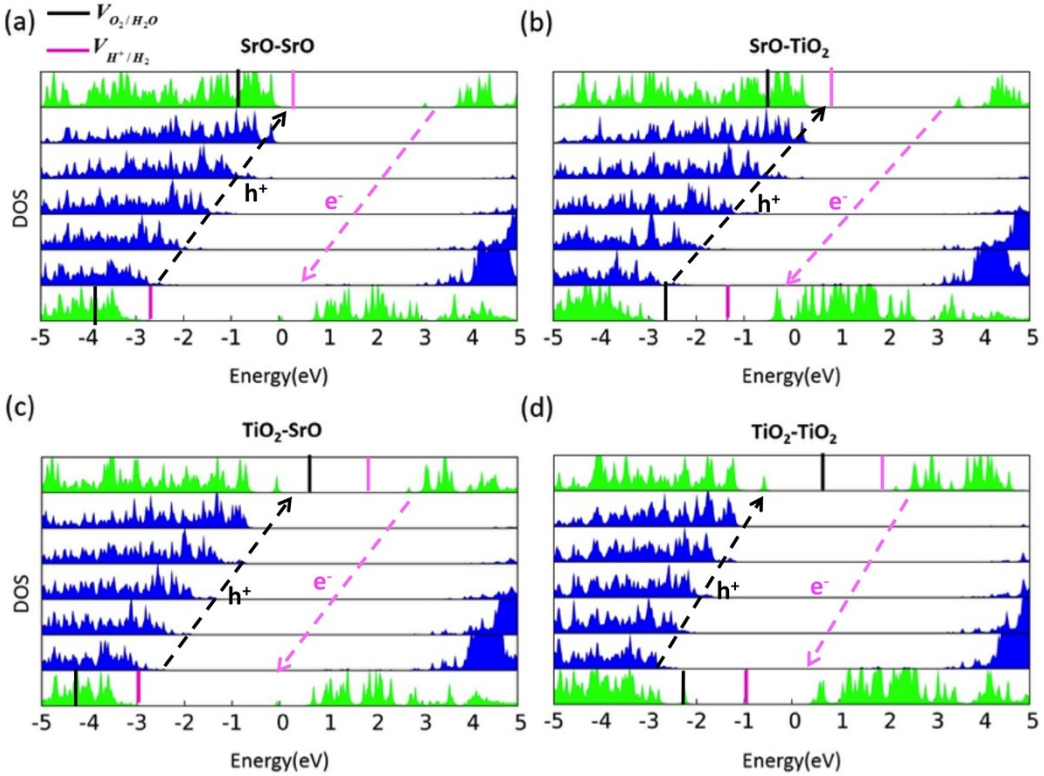


**Figure S5** DOS of four n-p-type STO/LAO/STO heterostructures with 5uc LAO and different STO terminations. The redox potential of $H_2O$ is marked by the black and pink lines.

## VI. The light absorption coefficient for n-p type STO/LAO/STO with 3% compressive strain.

Here what is shown is $TiO_2$-SrO type 4ucs STO/6ucs LAO/8ucs STO heterostructure. From the absorption figure, we can also see the absorption peak at infrared region, and the intensity is even stronger compared to that of 1uc STO/6uc LAO/1uc STO as shown by the blue curve in Fig. 4(c) in the main text.

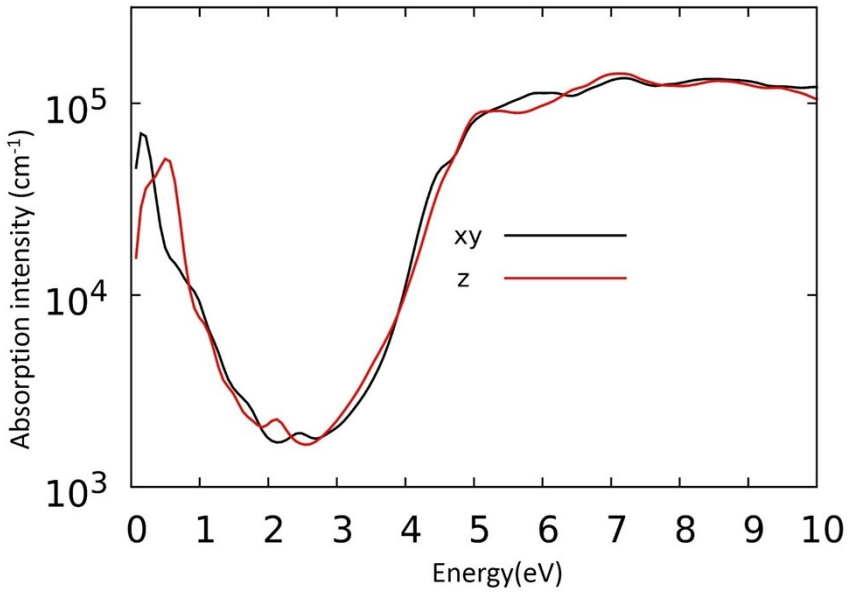


**Figure S6** Light absorption of $TiO_2$-SrO type 4ucs STO/6ucs LAO/8ucs STO heterostructure with 3% compressive strain.

**VII. The STO in the STO/LAO/STO heterostructure can be replaced by $TiO_2$ anatase.**

We have calculated the photoabsorption spectral of $TiO_2$/LAO/$TiO_2$ (001). Figure S7 (a) shows the atomic structure of $TiO_2$/LAO(3uc)/$TiO_2$. Similar with STO/LAO/STO, this heterostructure has a n-type $(LaO)^+/(TiO_2)^0$ interface and a p-type $(AlO_2)^-/(TiO_2)^0$ interface. In Figure S7 (b) we show the absorption spectral of this kind of heterostructure with different LAO thickness. It is shown that the heterostructures have a strong absorption peak in the range 0.2 ~ 0.5 eV when the LAO thickness exceeds 3 unit cells

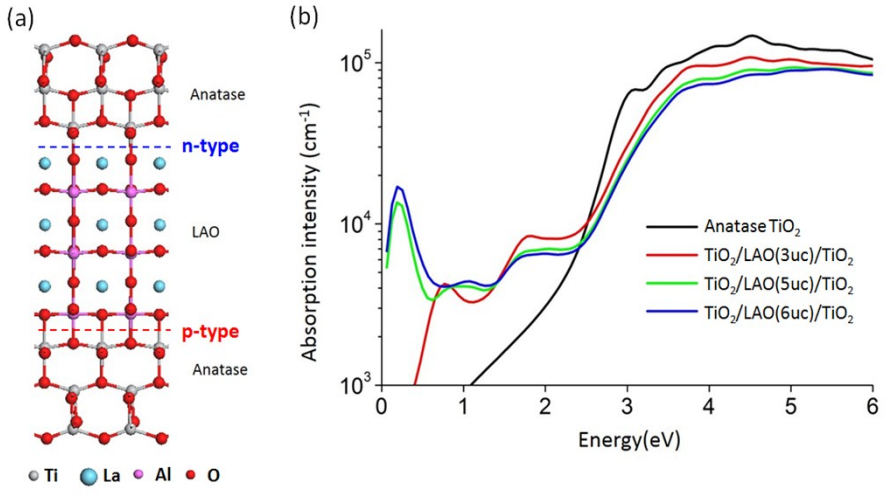


**Figure S7** The absorption intensity of $TiO_2$/LAO/$TiO_2$ heterostructures with 3uc, 5uc and 6 uc LAO.

**VIII. The debate on the origin of 2D electron gas at STO/LAO interface.**

There has been active debate about the underlying physical origin of 2D electron gas at

STO/LAO interface.[3-26] In the intrinsic charge reconstruction picture, the electron is transferred from the LAO surface to the interface above a critical LAO thickness to suppress the divergence of the electric potential associated with the polar field in the LAO overlayer (known as the "polar catastrophe").[6, 9, 16] Other possibilities for mitigating the polar catastrophe has also been proposed such as including redox screening[11-13] and interface intermixing[14-15]. In the redox screening model , the polar field in the LAO is expected to be minimal.[13-14] And in the interface intermixing model, the electrostatic potential in LAO is shifted.[27]

The main success of polar catastrophe scenario is that it very accurately predicts the critical thickness observed by Thiel et.al., which is a robust result that has been replicated in several groups.[5-6, 17-18] This critical thickness is also predicted by first principles calculations on stoichiometric STO/LAO slabs.[4, 19-20] Among many of the direct/indirect evidences which support the polar catastrophe scenario [3-6, 9, 17-25], Singh-Bhalla et.al. measured a bulid-in electric field of 80 mV/Å across LAO by carrying out tunneling measurements between the electron gas and metallic electrodes on $LaAlO_3$.[23] In addition, the capacitance measurements reveal the presence of induced dipole moment across the heterostructure.

It is helpful to convince the electric field in LAO predicted by first principles calculations can be realized in the experiments by comparing the calculated electrostatic potential with the experimental results. We estimated the electric field of LAO/STO with a 5 uc LAO based on the first principles calculations on stoichiometric STO/LAO slabs as shown in Figure 8 (a). The bulid-in electric field we obtained is 113 mV/Å, which agrees well with previous first principles investigations,[4, 19-20] however, larger than the experimental results. We believe this disagreement may be induced by the electrode attached to LAO surface. To simulate the real experimental conditions, we also calculated the electric field by attaching an Au over layer as the electrode as shown in Figure S8 (b). The field decreases to 83 mV/Å after Au capping. This results from the additional charge transfer from Au to STO near the LAO/STO interface. The calculated electric field of LAO/STO with Au electrode is in excellent agreement with the measurements by Singh-Bhalla et.al.[23] This supports that our proposed STO/LAO with minimal oxygen vacancies can be realized in the experiments and the electric field in LAO can be retained.

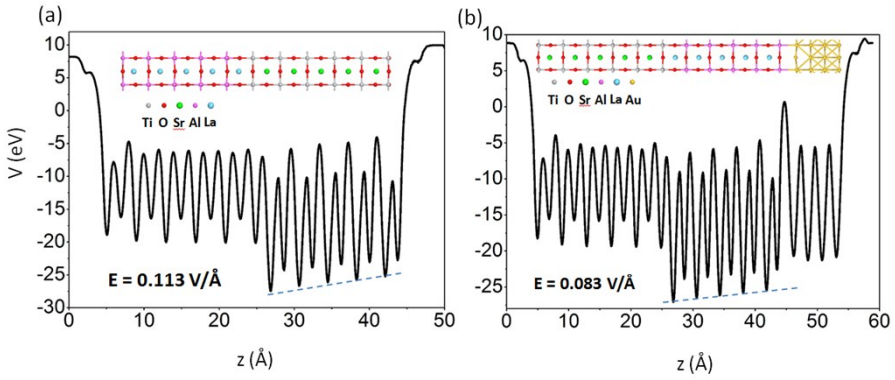


**Figure S8** The electrostatic potential (V) versus distance perpendicular to the (001) interface (z) of n-type STO/LAO heterostructure (5uc LAO) with and without Au electrode.

1. A. Kudo and Y. Miseki, *Chemical Society Reviews*, 2009, **38**, 253-278.
2. H.-C. Chen, C.-W. Huang, J. C. Wu and S.-T. Lin, *The Journal of Physical Chemistry C*, 2012, **116**, 7897-7903.
3. S. A. Pauli, S. J. Leake, B. Delley, M. Bjoerck, C. W. Schneider, C. M. Schlepuetz, D. Martoccia, S. Paetel, J. Mannhart and P. R. Willmott, *Phys. Rev. Lett.*, 2011, **106**, 036101.
4. J. Lee and A. A. Demkov, *Physical Review B (Condensed Matter and Materials Physics)*, 2008, **78**, 193104-193104.
5. C. Cancellieri, N. Reyren, S. Gariglio, A. D. Caviglia, A. Fete and J. M. Triscone, *Europhys. Lett*, 2010, **91**, 17004.
6. S. Thiel, G. Hammerl, A. Schmehl, C. W. Schneider and J. Mannhart, *Science*, 2006, **313**, 1942-1945.
7. H. Y. Hwang, Y. Iwasa, M. Kawasaki, B. Keimer, N. Nagaosa and Y. Tokura, *Nat. Mater.*, 2012, **11**, 103-113.
8. H. Chen, A. M. Kolpak and S. Ismail-Beigi, *Adv. Mater.*, 2010, **22**, 2881-2899.
9. N. Nakagawa, H. Y. Hwang and D. A. Muller, *Nat. Mater.*, 2006, **5**, 204-209.
10. C. Cen, S. Thiel, G. Hammerl, C. W. Schneider, K. E. Andersen, C. S. Hellberg, J. Mannhart and J. Levy, *Nat Mater*, 2008, **7**, 298-302.
11. W. Siemons, G. Koster, H. Yamamoto, W. A. Harrison, G. Lucovsky, T. H. Geballe, D. H. A. Blank and M. R. Beasley, *Phys. Rev. Lett.*, 2007, **98**, 196802.
12. G. Herranz, M. Basletic, M. Bibes, C. Carrétéro, E. Tafra, E. Jacquet, K. Bouzehouane, C. Deranlot, A. Hamzic, J.-M. Broto, A. Barthélémy and A. Fert, *Phys. Rev. Lett.*, 2007, **98**, 216803.
13. N. C. Bristowe, P. B. Littlewood and E. Artacho, *Phys. Rev. B*, 2011, **83**, 205405.
14. L. Qiao, T. C. Droubay, T. C. Kaspar, P. V. Sushko and S. A. Chambers, *Surf. Sci.*, 2011, **605**, 1381-1387.
15. P. R. Willmott, S. A. Pauli, R. Herger, C. M. Schlepütz, D. Martoccia, B. D. Patterson, B. Delley, R. Clarke, D. Kumah, C. Cionca and Y. Yacoby, *Phys. Rev. Lett.*, 2007, **99**, 155502.
16. A. Ohtomo and H. Hwang, *Nature*, 2004, **427**, 423-426.
17. D. G. Schlom and J. Mannhart, *Nat. Mater.*, 2011, **10**, 168-169.
18. M. Huijben, G. Rijnders, D. H. A. Blank, S. Bals, S. V. Aert, J. Verbeeck, G. V. Tendeloo, A. Brinkman and H. Hilgenkamp, *Nat. Mater.*, 2006, **5**, 556-560.
19. Z. S. Popovic, S. Satpathy and R. M. Martin, *Phys. Rev. Lett.*, 2008, **101**, 256801-256804.
20. R. Pentcheva and W. E. Pickett, *Phys. Rev. Lett.*, 2009, **102**, 107602.
21. M. L. Reinle-Schmitt, C. Cancellieri, D. Li, D. Fontaine, M. Medarde, E. Pomjakushina, C. W. Schneider, S. Gariglio, P. Ghosez, J. M. Triscone and P. R. Willmott, *Nat. Commun.*, 2012, **3**, 932.
22. C. Cancellieri, D. Fontaine, S. Gariglio, N. Reyren, A. D. Caviglia, A. Fete, S. J. Leake, S. A. Pauli, P. R. Willmott, M. Stengel, P. Ghosez and J. M. Triscone, *Phys. Rev. Lett.*, 2011, **107**, 056102.
23. G. Singh-Bhalla, C. Bell, J. Ravichandran, W. Siemons, Y. Hikita, S. Salahuddin, A. F. Hebard, H. Y. Hwang and R. Ramesh, *Nat. Phys.*, 2011, **7**, 80-86.
24. H. X. Liang, L. Cheng, X. F. Zhai, N. Pan, H. L. Guo, J. Zhao, H. Zhang, L. Li, X. Q. Zhang, X. P. Wang, C. G. Zeng, Z. Y. Zhang and J. G. Hou, *Sci. Rep.*, 2013, **3**, 1975.
25. A. Caviglia, S. Gariglio, N. Reyren, D. Jaccard, T. Schneider, M. Gabay, S. Thiel, G. Hammerl, J. Mannhart and J.-M. Triscone, *Nature*, 2008, **456**, 624-627.

26. T. Yajima, M. Minohara, C. Bell, H. Kumigashira, M. Oshima, H. Y. Hwang and Y. Hikita, *Nano Lett.*, 2015, **15**, 1622-1626.
27. N. C. Bristowe, P. Ghosez, P. B. Littlewood and E. Artacho, *J. Phys. Condens. Matter*, 2014, **26**, 143201.